A Fluorescence Study of the Adsorption of Water, Methanol, and Acetic Acid on an Activated Europium Ion-exchanged Mordenite

Tsuyoshi ARAKAWA,* Midori TAKAKUWA, and Jiro SHIOKAWA
Department of Applied Chemistry, Faculty of Engineering, Osaka University, 2-1 Yamadaoka, Suita, Osaka 565

(Received September 5, 1983)

The adsorption of water, methanol, and acetic acid on an activated Eu(III) ion-exchanged mordenite(Eu–M) has been studied by the measurement of the fluorescence of the Eu^{2+} ion which was produced by the dehydration at 500 °C. The emission peak of the Eu^{2+} ion sifted to a shorter wavelength on exposure to water and other simple molecules. The magnitude of the shift was correlated to the specific dielectric constant of the adsorbate. The quantum yield for the Eu^{2+} emission band after gas adsorption decreased in all cases. Also, the lifetime in the Eu^{2+}-adsorbate system was shorter than that in an activated Eu–M sample. The rate constants for the radiationless transitions were more sensitive to the nature of the adsorbates, and the order of the quenching power was $H_2O > D_2O > CH_3OH$.

The rare-earth ion-exchanged zeolites are well known as active catalysts for the cracking of fuel oil. The reduction-oxidation of the rare-earth ion in the zeolites, however, has apparently not been studied. We have now studied the fluorescence properties of rare-earth ion-exchanged zeolites in an attempt to clarify the catalytic properties of these compounds. Especially, we have found, from measurements of the fluorescence for europium ions, that Eu(III) is reduced to Eu(II) as Eu(III) ion-exchanged Y type zeolite or mordenite is evacuated at above 300 °C under a pressure of less than 10^{-2} Pa.1,2)

Physicochemical studies of the synthetic zeolites have been performed by several methods, *i.e.*, X-ray diffraction, electron resonance, infrared spectroscopy, reflectance spectroscopy, Mössbauer spectroscopy, magnetic susceptibility, and X-ray photoelectron spectroscopy, but the interpretation of the results and the establishment of firm conclusions are frequently difficult.3) Also, there have been a number of studies of the adsorption of various gases on the transition-metal ion-exchanged zeolites. Especially, the formation of a carbonyl, nitrosyl, or ammine complex in the zeolite has been reported on the basis of adsorption measurements and ESR spectroscopy.4–6) Although fluorescence spectroscopy is by no means a new technique, its application to the study of gas adsorption on rare-earth ion-exchanged zeolites as described here is new. In the case of Eu^{2+}-doped phosphors, it is well known that the emission band for the Eu^{2+} ion changes with the variation in the chemical environment around the Eu^{2+} ion, since the emission for the Eu^{2+} ion is due to a transition between $4f^7$ and $4f^65d$, and so the 5d electron will be most noticeably affected by the crystal field.7–9) Thus, after gas adsorption on an activated europium ion-exchanged mordenite (Eu–M), the peak position of the emission band for the Eu^{2+} ion can be expected to change with the adsorbates.10)

In this study, the unique features that have been observed only in an activated Eu–M during the adsorption of water, methanol, and acetic acid are presented.

Experimental

Materials. The Eu–M samples were prepared starting from Na-mordenite, which had been supplied by the Norton Company. The parent mordenite had the following composition; $Na_8(AlO_2)_8\cdot(SiO_2)_{40}\cdot 24H_2O$. This mordenite was ion-exchanged in an excess of a 0.02 M solution containing $EuCl_3$ (pH=4), washed, dried at 100 °C, and calcined in air at 450 °C. The exchanged mordenite was analyzed for europium by means of X-ray fluorometry and for sodium by means of flame photometry. The close correspondence between the decrease in the sodium content and the increase in the europium content indicated that a simple ion-exchange process had occurred. Thus, the exchanged level of the Eu^{3+} ion was 5.8%.

Water, dehydrated methanol, and acetic acid were degassed by the freeze-pump-thaw technique.

Adsorption Measurements. The adsorption experiments were performed on a silica balance, using a sample of 1.0×10^{-4} kg. The sensitivity was 10^{-7} kg. The apparatus of the gravimetric adsorption system, used in connection with a vacuum system, was similar to that described by Boudart *et al.*11) The pressure was monitored by a digital manometer (Validyne CD-23). The mordenite samples were evacuated for 2 h at room temperature before they were slowly heated at increments of 200 °C/h to 500 °C. The evacuation was then continued at 500 °C for 4 h. The adsorbate was introduced on a dehydrated sample at 25 °C.

Fluorescence and UV Experiments. The emission and excitation spectra were measured using a Shimadzu Recording Absolute Spectrofluorophotometer (RF-502) at room temperature. The UV spectra were taken with a Shimadzu UV-180 apparatus, using MgO as a reference. The particle size of the zeolite was in the 10^{-5}—10^{-4} m range, so that light scattering would be as uniform as possible. The UV spectra in the region from 200 to 400 nm were recorded using a glass filter (UV D-25), since the UV spectra in the region were affected by the fluorescence of a divalent europium ion, as will be described below. Prior to the adsorption, the sample in a quartz cell was dehydrated at 500 °C for 4 h under a pressure of 10^{-5} Torr(1 Torr=133.322 Pa), and then the adsorbate was introduced on dehydrated samples at 25 °C. The inlet adsorbate-gas pressure was the saturated vapor pressure at 25 °C. The quantum yield (Q_0) was decided using the following equation12);

$$Q_0 = Q_{\text{sample}} \times \frac{I_{\text{CaWO}_4:\text{Pb}}}{I_{\text{sample}}}, \tag{1}$$

where Q_{sample} is the photoluminescence outputs (PL) and is comparable to the PL of $CaWO_4$:Pb(NBS 1026), and where I_{sample} and $I_{\text{CaWO}_4:\text{Pb}}$ are the intensities obtained from the UV spectra.

Lifetime Measurement. The lifetimes were measured using a Nitrogen Laser (337 nm) with a lifetime of less than 5 ns. Also, for the measurement of the lifetimes the monochrometer was used in order to be capable of selecting the emission wavelength. The lifetimes were determined from the oscilloscope trace as the slope of log *I* vs. *t*.

Results

Adsorption Measurement. The adsorption of water, methanol, or acetic acid was rapid, and equilibrium was always attained within 1 or 2 h. The adsorption isotherms at 25 °C in Na-M and Eu-M are shown in Fig. 1. The amount of water adsorbed on Eu-M is more than that adsorbed on Na-M. For the adsorption of other species, the difference in the adsorbed amount between Eu-M and Na-M is small. The net amount of adsorption on europium was obtained from the difference between Eu-M and Na-M. In the case of water, this gave a quantity of adsorbed water per europium ion equal to 5.8 when the uptake at 10 Torr was plotted. Since the coordination number of water for the dehydrated europium chloride is 6,[13] the high uptake of water in Eu-M must be mainly due to the formation of the Eu^{2+}-aqua complex. In the case of CH_3OH, the observed CH_3OH/Eu ratio was about unity (1.3). The observed CH_3COOH/Eu ratio was also about unity (1.3). It is considered that, in the system of Eu-CH_3OH or Eu-CH_3COOH, the majority of Eu^{2+} ions exist in a state in which one molecule is coordinated to one Eu^{2+} ion in mordenite.

Fluorescence under Gas Adsorption. The compounds activated with an Eu^{2+} or Eu^{3+} ion generally exhibit fluorescence.[14,15] When Eu-M was degassed at 500 °C, the band emission for the Eu^{2+} ion(peak at 478 nm) and the emission lines for the Eu^{3+} ion, which had peaks at around 570($^5D_0$–$^7F_0$), 590($^5D_0$–$^7F_1$), and 620 nm ($^5D_0$–$^7F_2$), were observed.[2] However, the variation in the fluorescence for the Eu^{3+} ion under gas adsorption is not discussed in this paper, as the relative intensities of the emission lines were much smaller than that of the band emission for Eu^{2+} and the shift of the peak position for the emission band was not observed after the adsorption of gases. On the other hand, the band emission for the Eu^{2+} ion drastically changed after gas adsorption. Some typical excitation and emission spectra for the Eu^{2+} ion in mordenite are shown in Fig. 2. Curve 1 is the band emission for the Eu^{2+} ion which is produced in the course of evacuation at 500 °C. Curve 2 is the emission band when the dehydrated sample is exposed to water. The results of the other adsorbates are summarized in Table 1. The optimum excitation wavelength after gas adsorption was 355 nm in all cases. The emission band thus shifted to a shorter wavelength under gas adsorption.

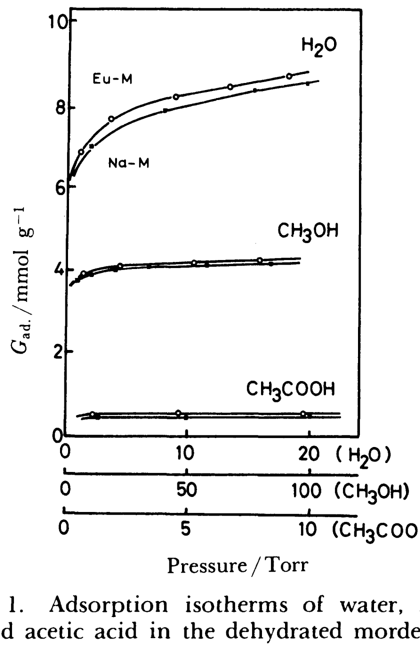

Fig. 1. Adsorption isotherms of water, methanol, and acetic acid in the dehydrated mordenite.

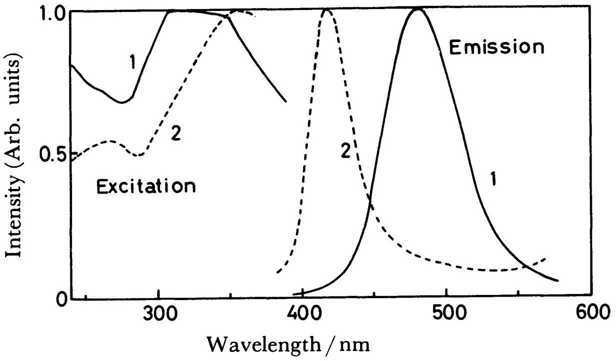

Fig. 2. The emission spectra for Eu^{2+} of Eu-M. (1) Degassed at 500 °C for 4 h and then cooled in vacuum to 25 °C. (2) After the introduction of water to (1).

TABLE 1. THE PEAK POSITION OF THE EMISSION BAND FOR THE Eu^{2+}-ADSORBATE SYSTEM IN MORDENITE

Adsorbate	Peak position (nm)
None	478
H_2O	419
D_2O	419
CH_3OH	418
CH_3COOH	415

UV Spectra. Figure 3 shows some typical absorption spectra before and after the adsorption of water and methanol. Although two bands appear after gas adsorption, the degree of splitting changes almost not at all from Eu-H_2O to Eu-CH_3COOH. On the other hand, the absorption edge of the spectra in the system for all Eu^{2+}-adsorbated molecules, which is the lowest energy edge (or the longest wavelength), almost agreed with the emission peak in Table 1.

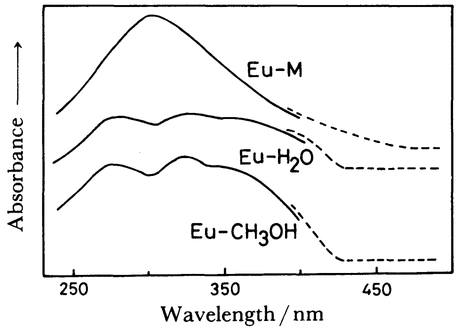

Fig. 3. Absorption spectra of Eu^{2+}-M, Eu^{2+}-H_2O and Eu^{2+}-CH_3OH system. The solid lines are the spectra with a glass filter (UV D-25).

Quantum Yield and Lifetimes. The quantum yield for the Eu^{2+} emission band after gas adsorption under the saturated vapor pressure at 25 °C is summarized in Table 2; it is then compared with the dehydrated sample. The quantum yield after gas adsorption decreases in all cases. That is, H_2O, CH_3OH, and CH_3COOH are quenchers. However, the degree of quenching is dependent on the adsorbates.

Only lifetimes longer than 5 ns could be measured. Thus, the lifetime for the adsorption of CH_3COOH could not be measured. The lifetimes were determined from the oscillograms. Although the oscillogram was composed of two parts (an initial increase in light intensity and then a decay), the results in Table 2 are for only the decreasing part of the picture; the increase was too short to be measured accurately. The decreasing part of the oscillogram represented an exponential decay in the systems of Eu^{2+}–H_2O and Eu^{2+}–D_2O. In an Eu^{2+}–CH_3OH system, although the light intensity decreased exponentially, it was proved that there were two lifetimes from the oscilloscope trace, the slope of log *I* *vs.* *t*. In all cases, the lifetime in the Eu^{2+}–adsorbated system is shorter than that in a dehydrated Eu–M. Although the influence of the concentration of an adsorbate on the lifetimes could not be examined as well as in a homogeneous system,[16] the luminescence decay rates in Eu^{2+}–CH_3OH must decrease with the increase in the number of methanol molecules coordinated to the Eu^{2+} ion. Therefore, it would seem that there are two sites where the coordination number of CH_3OH molecules for the Eu^{2+} ion are different from each other. This assumption would be appropriate since the value of CH_3OH/Eu^{2+} is not an integral number as described above.

TABLE 2. LIFETIMES AND QUANTUM YIELDS

Adsorbate	τ/ns	Q_0/%
None	1.1×10^3	0.9
CH_3OH	16,100	0.4
D_2O	7.2	0.2
H_2O	4.8	0.6
CH_3COOH	—	0.08

Discussion

Shift of Emission Peak. The emission for the Eu^{2+} ion is normally associated with the transitions from $4f^65d$ to $4f^7$ where $4f^65d$ is the excited state of Eu^{2+}. Two factors determine the wavelength of the emission band; the splitting of the 5d levels by the crystal field of the surrounding ligand ions and, on the other hand, the energy gap between the 4f ground state and the center of the gravity of 5d excited levels.[7,9] The existence of two peaks in Fig. 3 may be a result of the splitting of the 5d orbitals which increased after gas adsorption. That is, the shift of the emission peak after gas adsorption must be attributed to the fact that the adsorbate molecules are coordinated to an Eu^{2+} ion, as has been described above. Especially, in the Eu^{2+}–H_2O system, it was confirmed that the Eu^{2+}–aqua complex was formed after water adsorption. Moreover, we discussed the shift after gas adsorption. The relationship between the difference in the emission peak before and after gas adsorption and the specific dielectric constant (ε) of adsorbates is shown in Fig. 4. The magnitude of the shift ($\Delta\sigma_F$) is predicted by the approximate equation;[17]

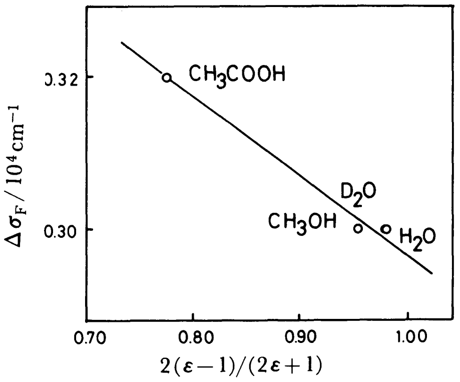

Fig. 4. The relationship between the dielectric constant of adsorbates and the shift of emission peaks for Eu^{2+}–adsorbated molecule in mordenite.

$$\Delta\sigma_F = \frac{2(\varepsilon-1)}{2\varepsilon+1}\alpha, \tag{2}$$

where α is the constant, which is determined by the photoexcited process of the Eu^{2+}–adsorbated molecule. Figure 4 well exhibits the relation of Eq. 2. As can be seen from the finding that the optimum excitation level after the adsorption rarely changed, the variation in the chemical environment around the Eu^{2+} ion under various condition of gas adsorption seems to be relatively unimportant in causing the variation in the excitation process. In Fig. 3, it may be seen that the lowest energy edge (or longest wavelength) almost agrees with the emission peak in Fig. 2. Therefore, it can qualitatively be mentioned that the shifts of the emission peak are dependent on the dielectric constant of the adsorbates, as the adsorbed molecules affect the dipole-dipole interaction Eu^{2+} ion in the dehydrated mordenite.

Rate Constant for Radiative and Radiationless Transitions. The information obtained from the lifetime and quantum-yield measurement enables us to calculate some of the rates of radiationless transitions. The quantum yield may be expressed as;

$$Q_0 = \frac{K_f}{K_f+K_i}, \tag{3}$$

where K_f is the radiative rate constant and K_i is the radiationless rate constant. Also, the observed lifetime, τ, is derived as the following equation;

$$\tau = \frac{1}{K_f+K_i}. \tag{4}$$

From Eqs. 3 and 4, we can calculate K_f and K_i. The results are given in Table 3. The radiationless constant, K_i, increases under the gas adsorption. Comparing the systems of Eu^{2+}–CH_3OH, Eu^{2+}–D_2O, and

Table 3. Rate constants for radiative (K_f) and radiationless (K_i) transitions

Adsorbate	$K_f/10^6\ s^{-1}$	$Q_0/\%$	$K_i/10^6\ s^{-1}$
None	0.09	0.9	0.9
CH_3OH	0.5, ~0	0.4	62, 10
D_2O	0.2	0.2	138
H_2O	1.2	0.6	207

Eu^{2+}-H_2O, the values of K_i are 62, 138, and 207 respectively. That is, the quenching rate constants are more sensitive to the nature of the adsorbates. The order of the quenching power is $H_2O(79)>D_2O(78)>CH_3OH(33)$. The values in parentheses are the dielectric constants. The order associates with the magnitude of the dielectric constant for the adsorbates.

It is considered that the results in this paper lead to a new method for investigating surface characteristics. Further detailed studies to investigate these interesting problems are now in progress.

We are grateful of Prof. H. Mikawa and Dr. Y. Shirota of Osaka University for their support of the measurements of the lifetimes.

References

1) T. Arakawa, T. Takata, G. Adachi, and J. Shiokawa, *J. Chem. Soc., Chem. Commun.*, **1979**, 453; *J. Luminescence*, **20**, 325 (1979).

2) T. Arakawa, T. Takata, M. Takakuwa, G. Adachi, and J. Shiokawa, *Mater. Res. Bull.*, **17**, 171 (1982).

3) For example, T. A. Egerton, A. Hagan, F. S. Stone, and J. C. Vickerman, *J. Chem. Soc., Faraday Trans.* 1, **68**, 723 (1972); K. Klier and M. Ralek, *J. Phys. Chem. Solids*, **29**, 951 (1968); D. H. Olson, *J. Phys. Chem.*, **72**, 4366 (1968).

4) E. F. Vansant and J. H. Lunsford, *J. Phys. Chem.*, **76**, 2860 (1972).

5) Y. Y. Huang, *J. Catal.*, **30**, 187 (1973); *J. Am. Chem. Soc.*, **95**, 6636(1973).

6) Y. Y. Huang and E. F. Vansant, *J. Phys, Chem.*, **77**, 663 (1973).

7) F. M. Ryan, W. Lehmann, D. W. Feldman, and J. Murphy, *J. Electrochem. Soc.*, **121**, 1475 (1974).

8) H. A. Weakliem, *Phys. Rev., B*, **6**, 2743 (1972).

9) D. S. McClure and Z. Kiss, *J. Chem. Phys.*, **39**, 3251 (1963).

10) T. Arakawa, M. Takakuwa, and J. Shiokawa, *Chem. Lett.*, **1982**, 999.

11) Y. Y. Huang, J. E. Benson, and M. Boudart, *Ind. Eng. Chem., Fundam.*, **8**, 346 (1969).

12) J. N. Denas and G. A. Crosby, *J. Phys. Chem.*, **75**, 991 (1971).

13) N. K. Belškii and Yu. T. Struchkov, *Sov. Phys, Crystallogr.*, **10**, 15 (1965).

14) G. Blasse, W. L. Wanmaker, J. W. terVrugt, and A. Brill, *Philips Res. Reports*, **23**, 189 (1968).

15) G. Blasse and A. Brill, *Philips Tech. Rev.*, **31**, 304 (1970).

16) Y. Hass and G. Stein, *J. Phys. Chem.*, **75**, 3668, 3677 (1979).

17) Y. Ooshika, *J. Phys. Soc. Jpn*, **9**, 594 (1954).